Electronic Supporting Information for

Effect of twisted molecular geometry on the solid-state emissions of an anthracene fluorophore

G. Gogoi and R. J. Sarma*

Department of Chemistry, Gauhati University, Guwahati, 781014 Assam, India

E-mail: rjs@gauhati.ac.in, rupam.sarma@gmail.com

Table of Contents

1. General experimental techniques.

All chemicals were commercially available from Sigma-Aldrich or Merck (India) and used as received. Solvents for spectroscopic experiments were distilled under nitrogen atmosphere before use. All ^{1}H and ^{13}C NMR were measured on a 300 MHz Bruker spectrometer, and reported in δ/ppm. The absorption spectra were recorded on a Shimadzu UV-vis spectrophotometer (Model UV-1800), and fluorescence spectra were recorded using a Hitachi F2500 fluorimeter

2. Synthetic Procedures

Synthesis of A-4OH: Compound **A-4OH**was synthesized by reacting anthracene-9-aldehyde with 4-hydroxylbenzohydrazide, according to Scheme 1:

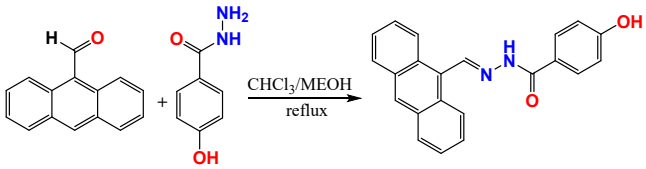

Scheme 1: Synthesis of **A-4OH**

Synthesis of ligand A-4OH. To a solution of anthracene-9-aldehyde (0.206 g,1.0 mmol) in chloroform (5 mL), was added 4-benzoylhydrazide (0.242g,1.0 mmol) in methanol (5 mL) and the mixture was stirred at 80°C for 8 h. When the reaction was complete, the reaction mixture was concentrated under vacuum and desired compound precipitated out. This residue was rinsed with methanol(5 mL)to afford a yellow-coloured product**A-4OH**. Yield ~ 84%; ^{1}H NMR(300MHz, DMSO-d_6) δ_H 11.95 (1H, s, amide NH),10.33 (1H, s, -OH), 9.60 (1H, s, N=CH), 8.74 (1H, s, Ar-H), 8.71-8.69 (2H, d, Ar-H), 8.14-8.12 (2H, d, Ar-H), 7.92-7.89 (2H, d, Ar-H), 7.64-7.56 (4H, m, Ar-H), 6.93-6.90 (2H, d, Ar-H). ^{13}C NMR (75MHz, DMSO-d_6) 162.50, 160.57, 145.90, 130.76, 129.60, 129.40, 128.86, 127.02, 125.45, 125.09, 124.76, 123.63, 114.99. ES-MS: m/z 341.13 calc. for ($M+H^+$).

Crystal formation procedure

A-4OH-G: Approximately 0.5 mg of C were taken in a glass vial and dissolved in 200 µL THF. The glass vial was capped for slow evaporation of the solvent. After 2-3 weeks green emissive crystals were obtained.

A-4OH-NE: A very concentrated solution of **A-4OH** in distilled N,N-dimethyl formamide (1mg/50µL) was prepared and kept for crystallization on a watch glass. After 1 day block like crystals were obtained.

A-4OH-O: 3 mg of **A-4OH** were taken in a glass sample vial and dissolved in 1 mL Methanol and DMSO separately. After 1-2 week prism like orange emissive crystals were obtained.

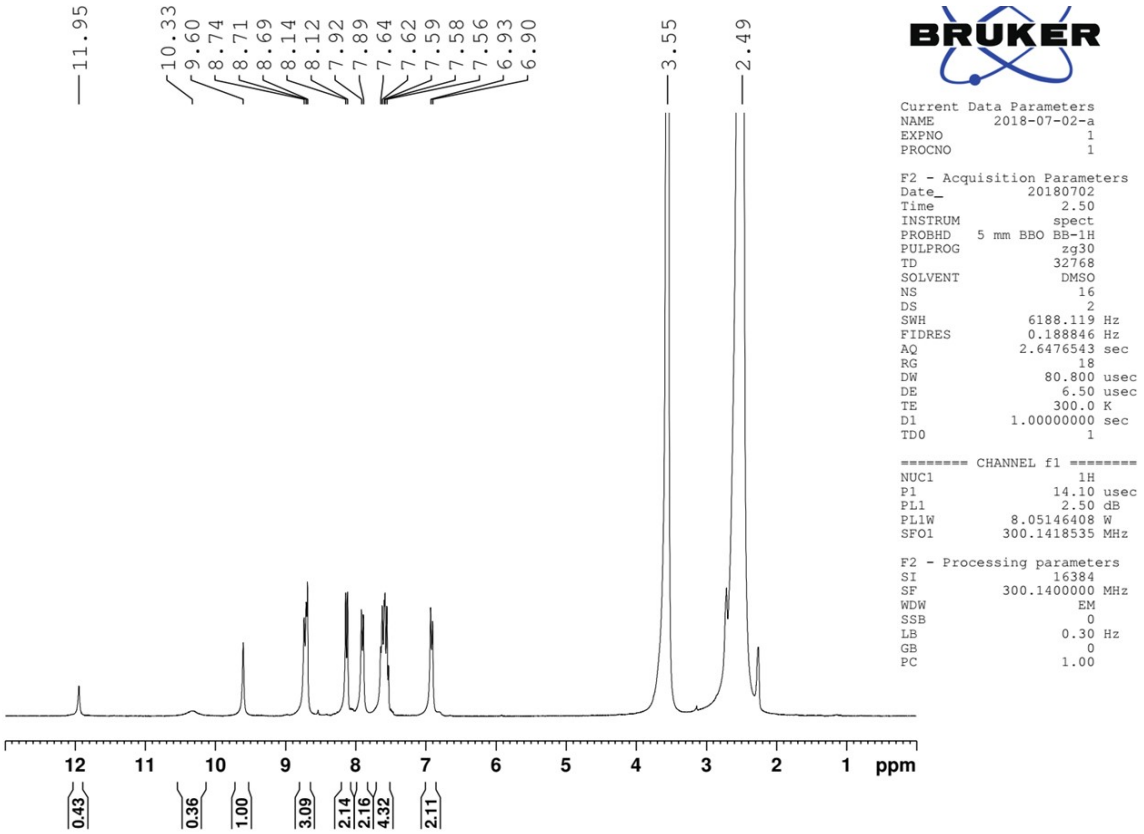

Figure S1: ^{1}H NMR spectra of **A-4OH** in DMSO-d_6

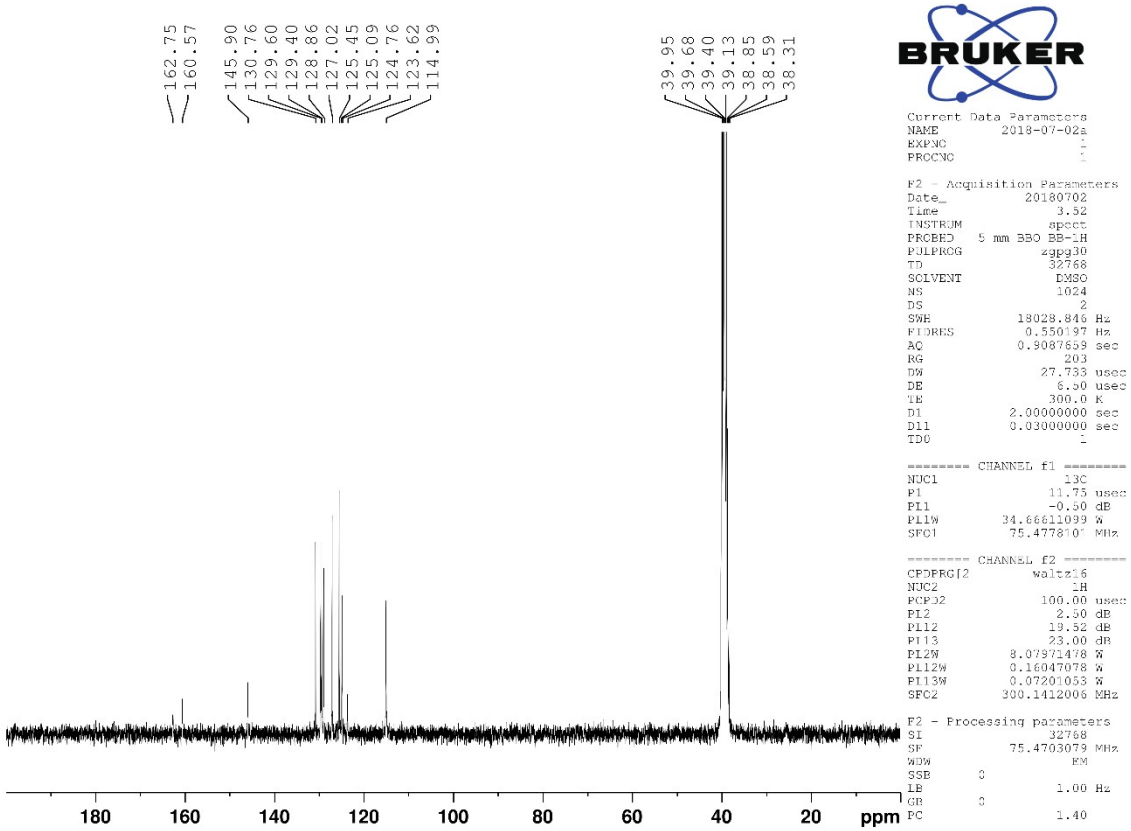

Figure S2: ^{13}C NMR spectra of **A-4OH** in DMSO-d_6

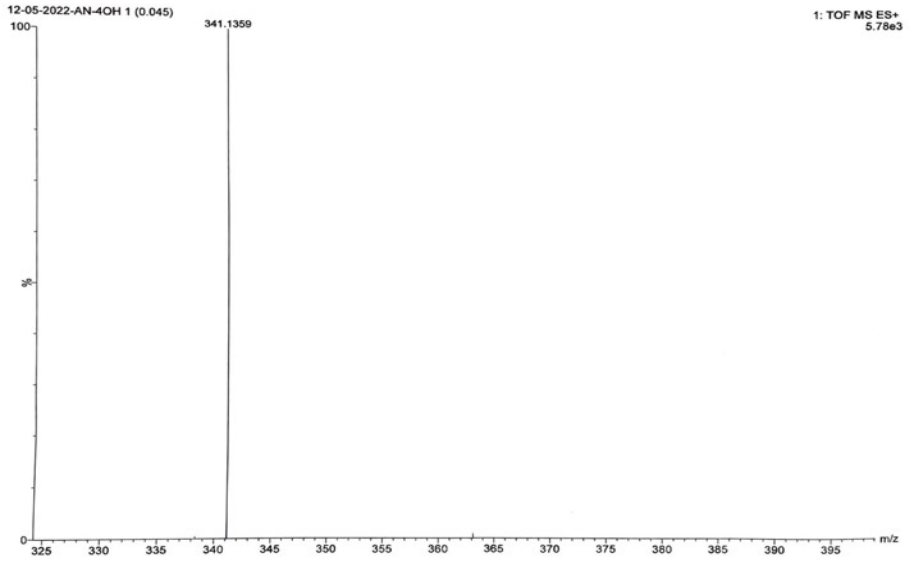

Figure S3: ES-MS spectra of **A-4OH**

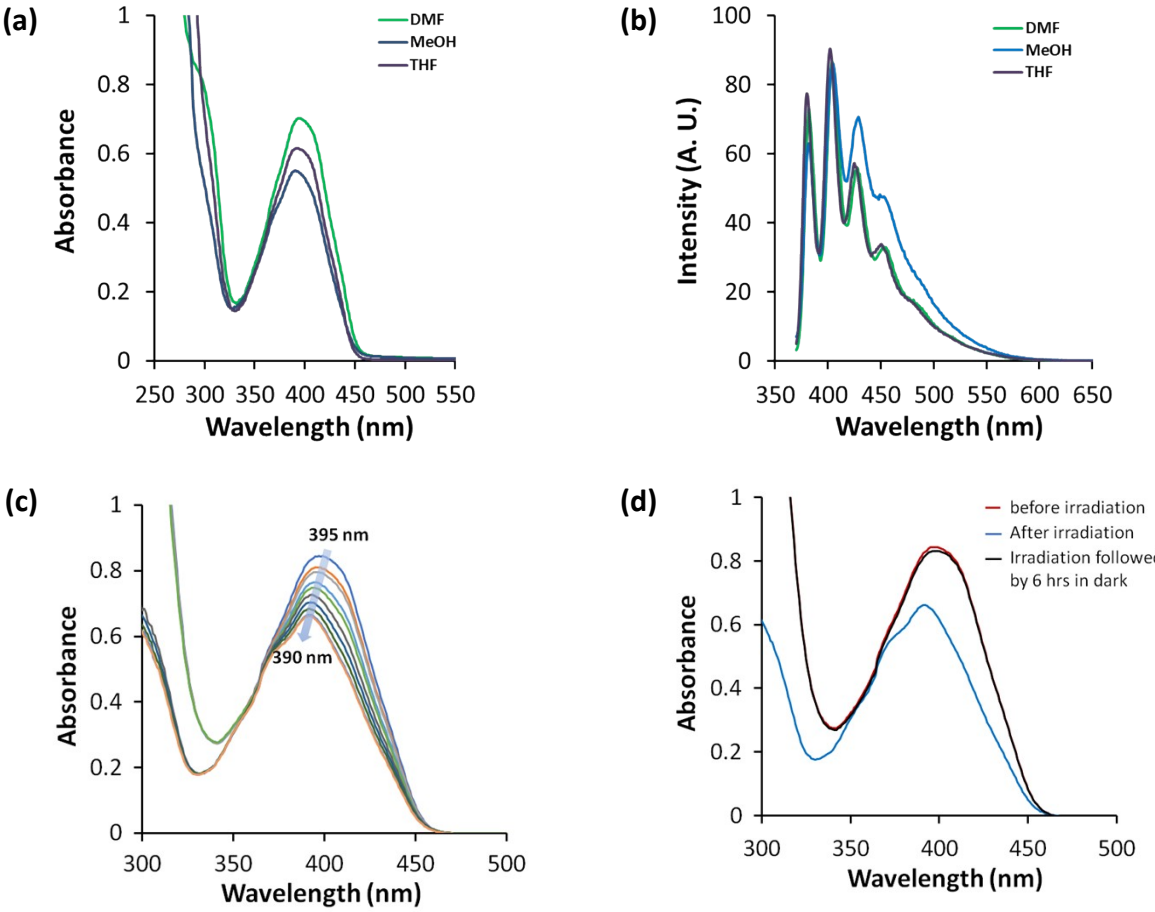

Figure S4: Solvent dependent (a) UV-vis, and (b) fluorescence spectra of **A-4OH** (conc. <0.1mM); (c) Changes in the UV-vis spectra of **A-4OH** in DMF arising from photochemical *trans-cis* isomerization following exposure to 365 nm UV-light (recorded at intervals of 1 min); (b) Thermal *cis–trans* isomerization which occurs spontaneously in the dark.

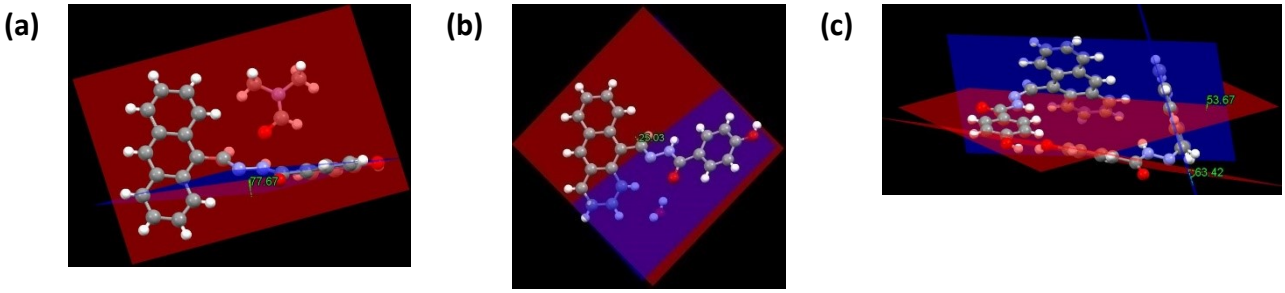

Figure S5: Relative orientations of the anthracene and the hydroxy phenyl group in (a) **A-4OH-NE**; (b) **A-4OH-O**; and (c)**A-4OH-G**.

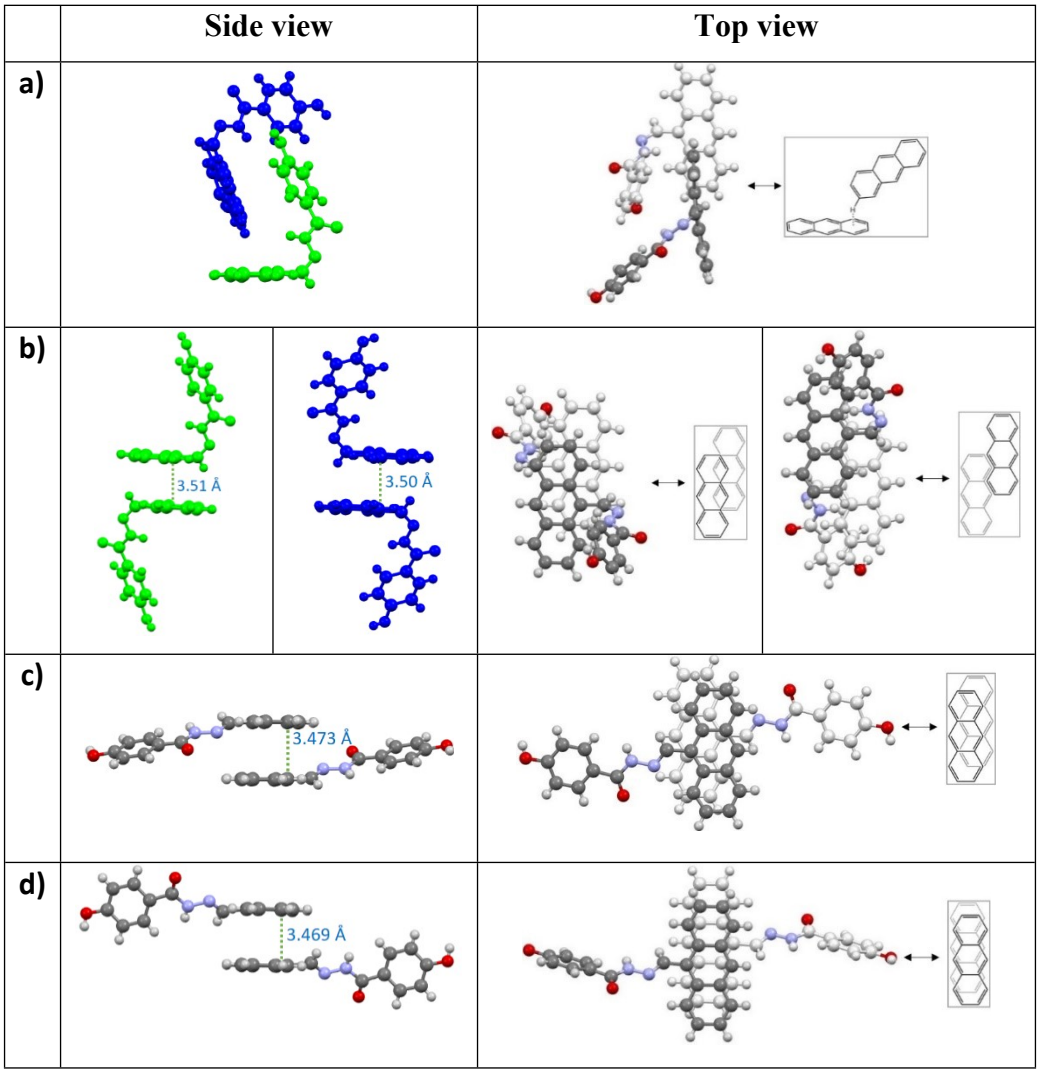

Figure S6: Side view and top view stacking structures of **A-4OH** crystals showing (a) CH–π interaction between two symmetric independent units of **A-4OH-G**, (b) π–π interaction between two symmetric related units of **A-4OH-G**, (c) and (d) π–π interaction between anthracene motifs of **A-4OH-O** and **A-4OH-NE** respectively; (inset: top view stacking mode of anthracene dimer)

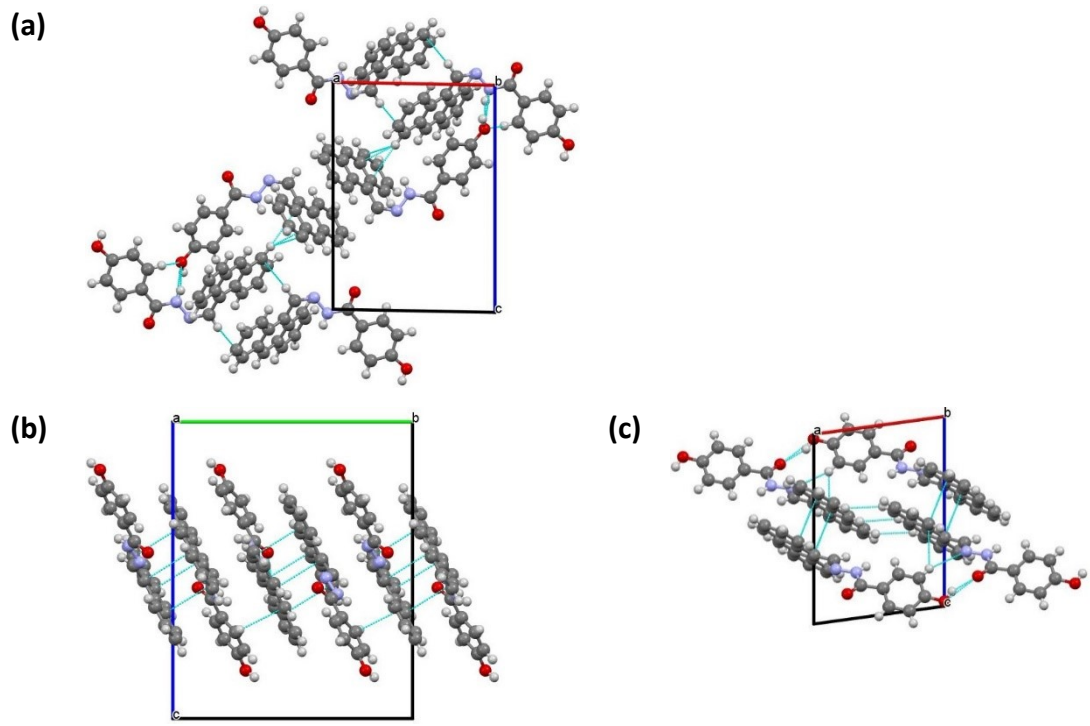

Figure S7: Packing structures showing aromatic π–π interactions of (a) **A-4OH-G** along b-axis, (b) **A-4OH-O** along a-axis, and (c) **A-4OH-NE** along b-axis

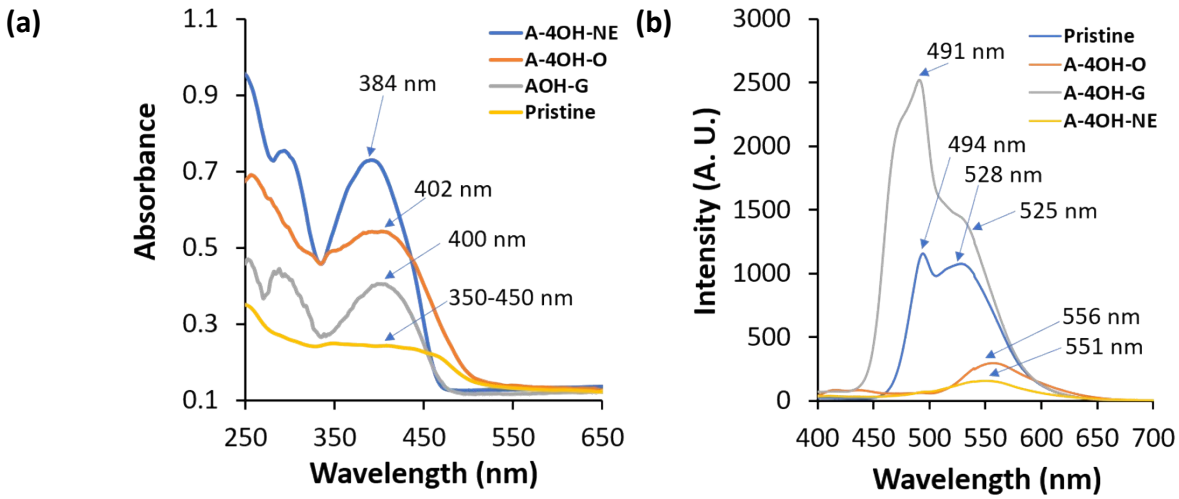

Figure S8: Solid state (a) UV-vis, and (b) fluorescence spectra of **A-4OH-NE**, **A-4OH-O**, **A-4OH-G** and pristine form

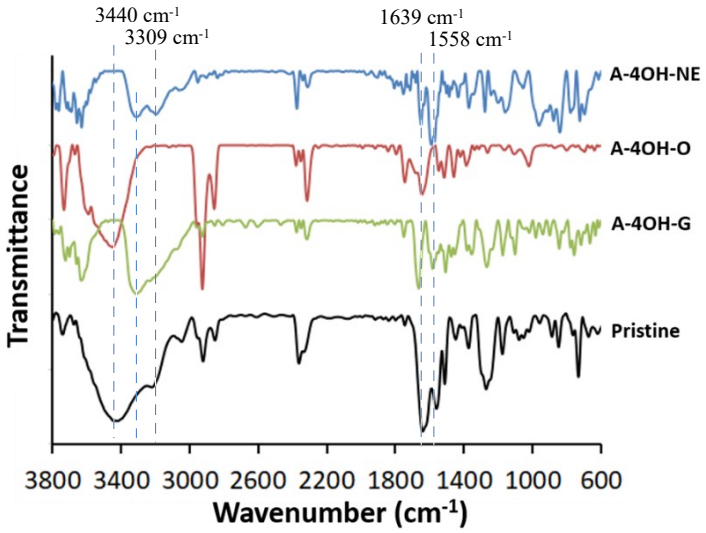

Figure S9: Overlay of the FT-IR spectra of pristine form**, A-4OH-NE, A-4OH-O** and **A-4OH-G** forms.

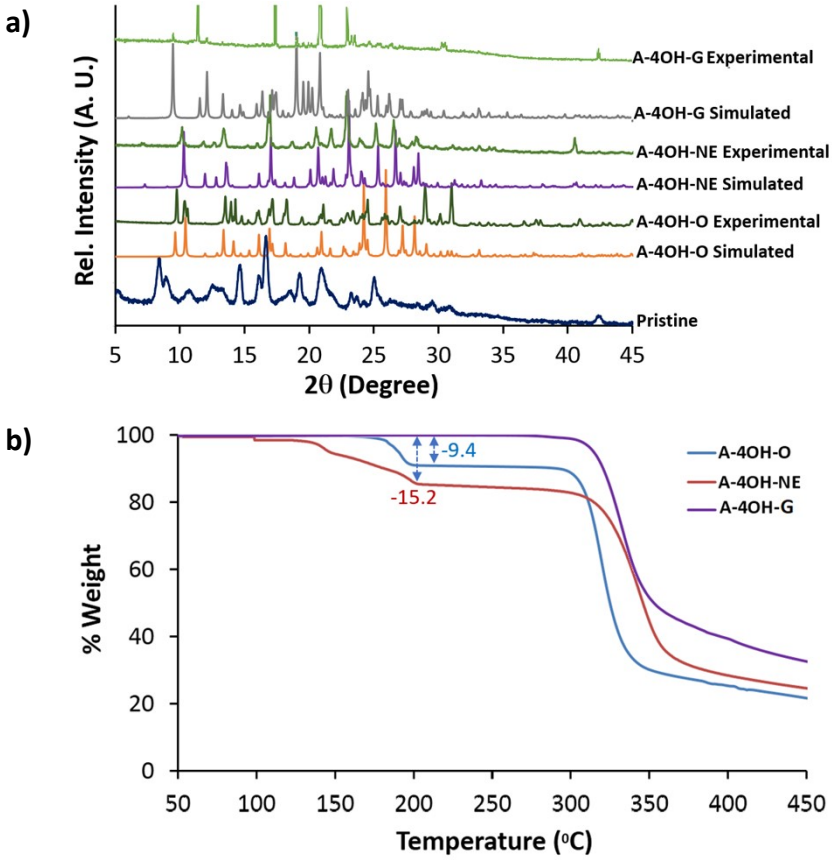

Figure S10: (a)Simulated and experimental powder XRD pattern of **A-4OH-NE**, **A-4OH-O**, **A-4OH-G** and PXRD pattern of pristine form;(b)TGA graph of **A-4OH-NE**, **A-4OH-O** and **A-4OH-G.**

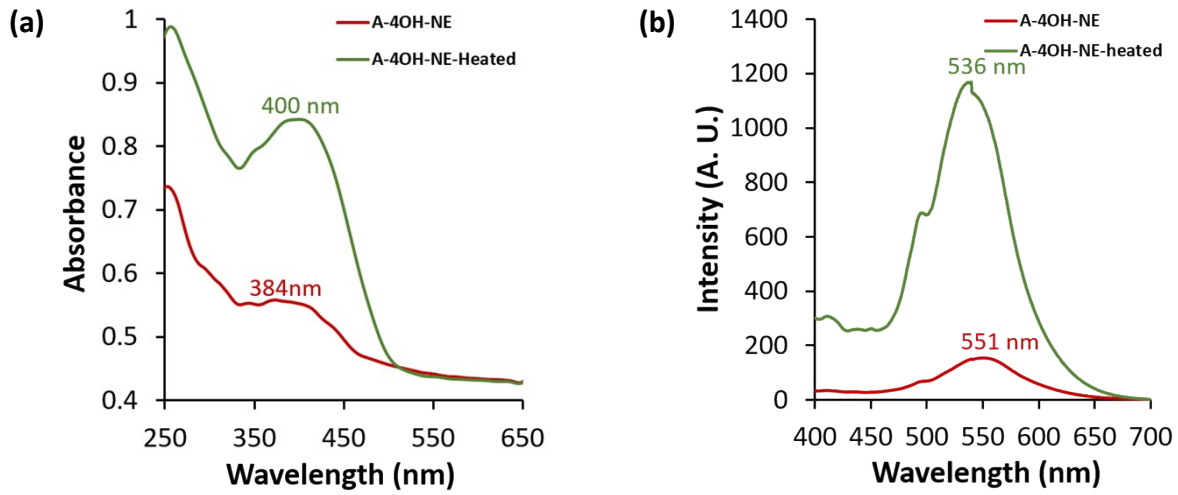

Figure S11: Solid state (a) UV-visible and (b) fluorescence spectra of **A-4OH-NE** before and after thermal stimulation.

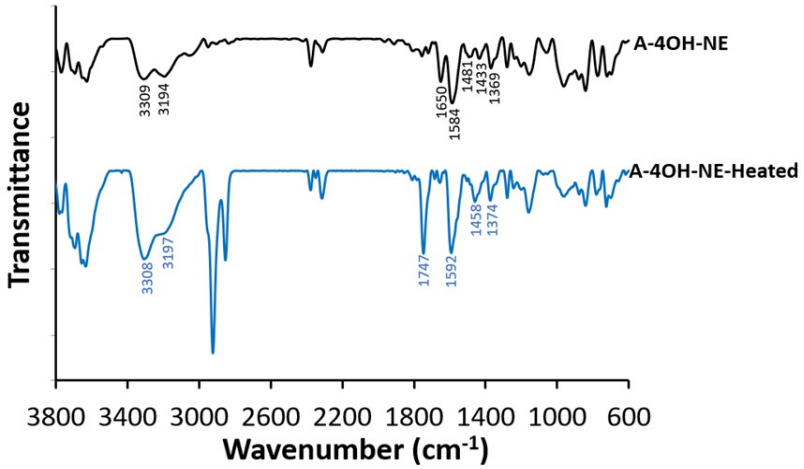

Figure S12: (a) Overlay of the (a) FTIR spectra and (b) thermogravimetric analysise of **A-4OH-NE** before and after thermal stimulation, viz. **A-4OH-F**.

a)

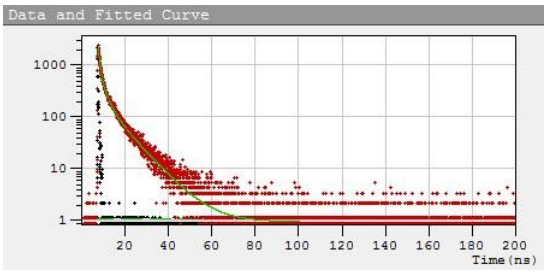

❖ **Exponential Components Analysis (Reconvolution)**

Fitting range : [140; 2050] channels
χ^2 : 1.002

	B_i	ΔB_i	f_i (%)	Δf_i (%)	τ_i (ns)	$\Delta\tau_i$ (ns)
1	0.4997	0.0428	46.125	7.262	0.591	0.042
2	0.0620	0.0032	25.591	1.474	2.643	0.015
3	0.0193	0.0008	28.284	1.173	9.400	0.002

Shift : -0.694 ns (± 1.002 ns)
Decay Background : 0.943 (± 0.076)
IRF background : 0

b)

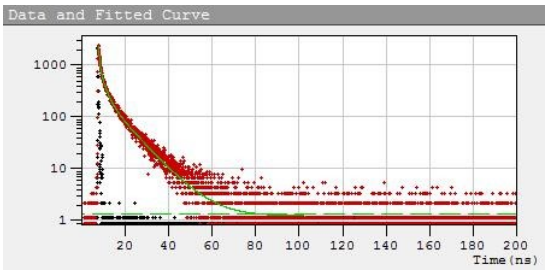

❖ **Exponential Components Analysis (Reconvolution)**

Fitting range : [139; 2100] channels
χ^2 : 1.001

	B_i	ΔB_i	f_i (%)	Δf_i (%)	τ_i (ns)	$\Delta\tau_i$ (ns)
1	0.2306	0.0111	21.396	5.331	0.432	0.087
2	0.0615	0.0017	31.472	1.022	2.384	0.013
3	0.0229	0.0006	47.132	1.185	9.594	0.001

Shift : -0.098 ns (± 0.860 ns)
Decay Background : 1.213 (± 0.076)
IRF background : 0

Figure S13: Time resolved photoluminescence spectra of (a) **A-4OH-NE** and (b) **A-4OH-NE** heated form

a)

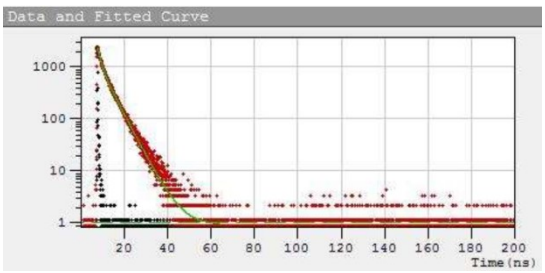

❖ **Exponential Components Analysis (Reconvolution)**

Fitting range : [139; 1300] channels
χ^2 : 1.003

	B_i	ΔB_i	f_i (%)	Δf_i (%)	τ_i (ns)	$\Delta\tau_i$ (ns)
1	0.2287	0.0568	33.251	8.614	1.433	0.015
2	0.1200	0.0083	66.749	4.609	5.483	0.001

Shift : -1.074 ns (± 7.766 ns)
Decay Background : 0.922 (± 0.113)
IRF background : 0

b)

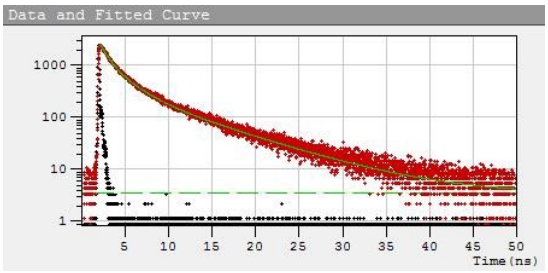

❖ **Exponential Components Analysis (Reconvolution)**

Fitting range : [154; 4096] channels
χ^2 : 1.176

	B_i	ΔB_i	f_i (%)	Δf_i (%)	τ_i (ns)	$\Delta\tau_i$ (ns)
1	0.0538	0.0022	18.481	2.366	0.768	0.067
2	0.0376	0.0018	38.178	2.123	2.273	0.016
3	0.0122	0.0004	43.341	1.348	7.948	0.002

Shift : -0.103 ns (± 2.207 ns)
Decay Background : 3.259 (± 0.156)
IRF background : 0.100

c)

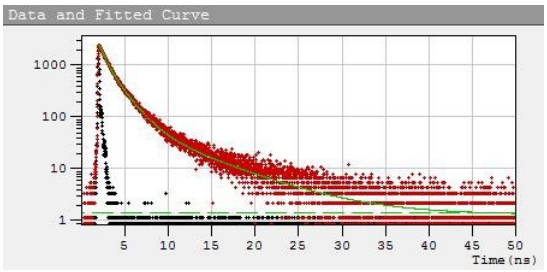

❖ **Exponential Components Analysis (Reconvolution)**

Fitting range : [147; 4096] channels
χ^2 : 1.119

	B_i	ΔB_i	f_i (%)	Δf_i (%)	τ_i (ns)	$\Delta\tau_i$ (ns)
1	0.0507	0.0009	19.500	2.830	0.490	0.063
2	0.0482	0.0008	63.668	1.404	1.681	0.008
3	0.0033	0.0002	16.832	0.787	6.591	0.003

Shift : -0.049 ns (± 0.870 ns)
Decay Background : 1.292 (± 0.072)
IRF background : 0.100

Figure S14: Time resolved luminescence spectra of (a) **A-4OH-G**, (b) **A-4OH-O** and (c) pristine form.

Table S1. Comparison of the average fluorescence lifetime of **A-4OH-NE, A-4OH-NE (heated), A-4OH-O** and pristine sample							
	f1	**τ1**	**f2**	**τ2**	**f3**	**τ3**	**ns**
A-4OH-NE	0.46125	0.59	0.25598	2.643	0.28284	9.4	3.604
A-4OH-NE (heated)	0.21396	0.432	0.31472	2.384	0.47132	9.594	5.364
A-4OH-O	0.18481	0.768	0.38178	2.273	0.43341	7.948	4.454
A-4OH-G	0.33251	1.433	0.66749	5.483			4.136
Pristine	0.195	0.49	0.63668	1.681	0.16832	6.591	2.275

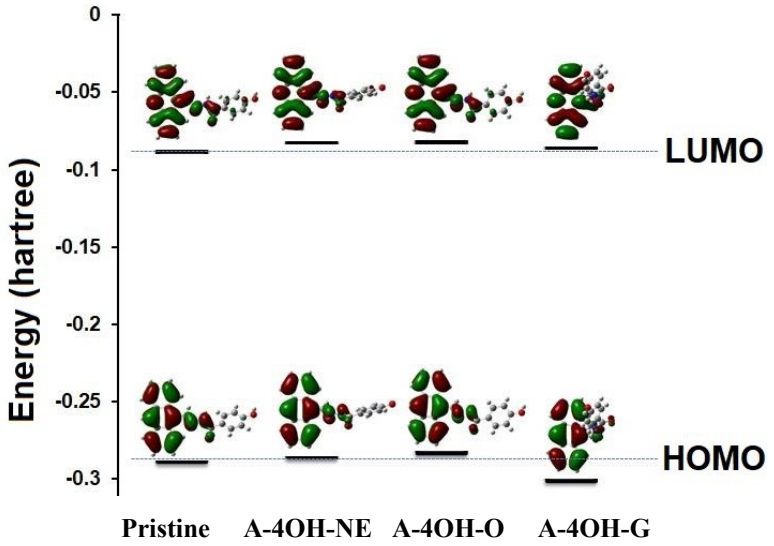

Figure S15: HOMO-LUMO energy diagram of **A-4OH**, **A-4OH-NE**, **A-4OH-O** and **A-4OH-G** as obtained from DFT calculations (using B3LYP/6-31G level of theory).

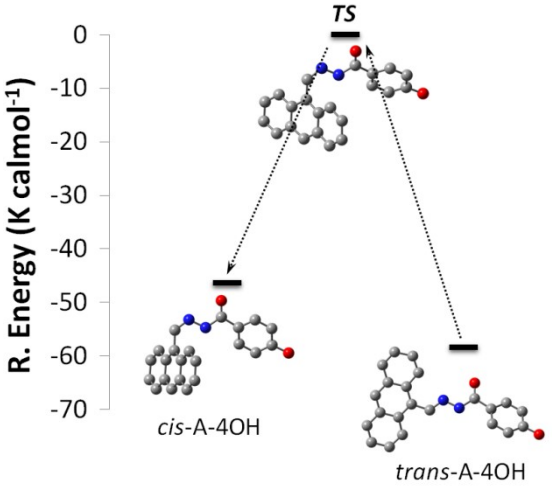

Figure S16. Calculated structures of the transition states (TS) for the photochemically induced *trans-cis* isomerisation of **A-4OH**, corresponding to an energy barrier of 62.0 kcal/mol.

Table S2. Crystallographicdata and refinement parameters of **A-4OH-NE**, **A-4OH-O** and **A-4OH-G**

	A-4-OH-NE	**A-4OH-O**	**A-4OH-G**
Empirical formula	C_{25} H_{23} N_3 O_3	C_{22} H_{18} N_2 O_3	$C_{44}H_{32}$ N_4 O_4
Formula weight	413.48	358.38	680.73
Temperature	296(2) K	296(2) K	296(2) K
Wavelength	0.71073 Å	0.71073 Å	0.71073 Å
Crystal system	Triclinic	Orthorhombic	Triclinic
Space group	*P*–1	*P*bca	*P*–1
Unit cell dimensions	a = 8.5226(3) Å, b = 10.0347(4) Å, c = 12.5476(5) Å, α = 77.009(2)° β = 81.678(2) ° γ = 86.510(2) °	a = 12.5066(4)Å, b = 14.8096(5)Å, c = 18.3306(7)Å, α = 90° β = 90° γ = 90°	a = 11.3394(8) Å, b = 11.3450(8) Å, c = 14.9825(10) Å, α = 77.424(5)° β = 86.116(4)° γ = 67.045(4)°
Volume	1034.17(7) Å	3395.2(2)Å	1731.9(2)Å
Z	2	8	2
Density (calculated)	1.184	1.402	1.305
Absorption coefficient	0.089	0.094 mm^{-1}	0.085
F(000)	436.2039	1504	712
Theta range for data collection	2.95 to 29.08°	2.404to 29.082°	1.393° to 26.596°
Index ranges	-11<=h<=11, -13<=k<=13, -17<=l<=17	-17<=h<=11, -20<=k<=20, -25<=l<=21	-14<=h<=14, -14<=k<=14, -18<=l<=17
Reflections collected	20541	18823	27578
Independent reflections	[R(int) =]	[R(int) =]	[R(int) =]
Completeness to theta25.242°	25.242°	25.242°	25.242°
Refinement method	Full-matrix least-squares on F^2	Full-matrix least-squares on F^2	Full-matrix least-squares on F^2
Data / restraints / parameters	5514 / 0 / 283	4469 / 0 / 273	7160 / 0 / 486
Goodness-of-fit on F^2	1.0544	1.063	1.061
Final R indices [I>2sigma(I)]	R1 =0.0508, wR2 = 0.1411	R1 =0.0466, wR2 = 0.1152	R1 =0.0723, wR2 =0.1724
R indices (all data)	R1 =0.0708, wR2 = 0.1589	R1 =0.0678, wR2 =0.1278	R1 =0.1413, wR2 =0.2116
Largest diff. peak and hole	e.$Å^{-3}$	e.$Å^{-3}$	e.$Å^{-3}$